Forbidden transitions in the ^{48}Ca(d,p)^{49}Ca reaction*

W. D. Metz,[†] W. D. Callender, and C. K. Bockelman

Wright Nuclear Structure Laboratory, Yale University, New Haven, Connecticut 06520

(Received 19 December 1974; revised manuscript received 16 June 1975)

In a measurement of the angular distribution of proton groups from the ^{48}Ca(d,p)^{49}Ca reaction at $E_d = 20$ MeV, particular emphasis is placed on the observation of seven weak transitions to states below 5 MeV excitation. These distributions are analyzed using distorted-wave Born-approximation (DWBA) parameters fixed by fitting, at $E_d = 13.0$, 16.0, and 19.3 MeV, the angular distributions of the elastically scattered deuterons and the protons populating the single-particle $2p_{3/2}$, $2p_{1/2}$, and $1f_{5/2}$ states. The DWBA model also fits the (d,p) data of other investigators at $E_d = 7.0$ and 10.0 MeV. The same model is then applied to the seven weak transitions, for which earlier data are available at 7.5 and 10.0 MeV in addition to the new $E_d = 20$ MeV data. New partial angular distributions at 9.0 MeV are helpful in resolving some discrepancies. For three of the weak transitions, older l assignments are confirmed, for two of them new l assignments are made, and for two transitions the observed behavior is incompatible with any reasonable DWBA model. All seven transitions can be explained as populating 2p-1h states formed by coupling a neutron to excited states of the ^{48}Ca core.

NUCLEAR REACTIONS ^{48}Ca(d,p), $E_d = 9, 13, 16, 19.3, 20$ MeV; measured $\sigma(E_p, \theta)$; deduced levels, J, π, l, spectroscopic factors. Enriched target.

I. INTRODUCTION

The validity of the simple shell model has been investigated extensively in medium-weight nuclei near the doubly closed-shell nucleus ^{40}Ca. Although the dominant transitions in this region populate states that are reasonably well described by the shell model, many states not predicted by the shell model also appear, demanding more sophisticated models that introduce extra degrees of freedom to account for the extra states. There is evidence from a variety of single-nucleon transfer reactions[1-4] that the prominent features of nuclei near ^{48}Ca may be simpler, in that they may be well described by the shell model. However, some departures from the simple shell model have been noted in ^{49}Ca; Canada, Ellegaard, and Barnes[5] have suggested that certain of these deviations may be explained by simple couplings of single-particle excitations to excited states of the ^{48}Ca core.

Unfortunately, the scarcity of nuclides near ^{48}Ca with lifetimes long enough to be used as targets precludes as extensive an investigation as has been possible for the $A = 40$ region. Therefore it has been necessary to refine the early nucleon-transfer measurements proceeding from the only stable target available, ^{48}Ca. Measurements of the ^{48}Ca(d,p)^{49}Ca reaction by Kashy, Sperduto, Enge, and Buechner[1] at 7.0–7.5 MeV deuteron energy established the existence of strong transitions to the $2p_{3/2}$, $2p_{1/2}$, and $1f_{5/2}$ single-particle states predicted by the simple shell model (allowed transitions) and also of weaker transitions to non-single-particle states (forbidden transitions). For the $2p$ states these initial investigations were extended by others to higher and lower deuteron energies. Belote, Dorenbusch, and Rapaport[6] remeasured the ground-state $2p_{3/2}$ transition at 7.0 and 7.2 MeV, and Anderson, Hansen, Chapman, and Hinds[7] extended that measurement to $E_d = 10$ MeV. Both $2p$ transitions were studied by Brown, Denning, and Macgregor,[8] again at $E_d = 10$ MeV. The Coulomb stripping experiments of Bogaards and Roy[9] and of Rapaport, Sperduto, and Salomaa[10] confirmed the single-particle nature of these transitions.

The energies of the forbidden transitions seen by Kashy *et al.*[1] were confirmed to good accuracy by Erskine, Marinov, and Schiffer.[2] Recently Brown, Denning, and Haigh[11] have reported high-resolution proton angular distributions observed with 10 MeV deuterons that confirm and extend many of the conclusions of Ref. 1. Both experiments (Refs. 1 and 11) focus on the bound states ($E_{\text{ex}} < 5.14$ MeV) that are weakly excited in the d,p reaction. As in the case of the strong transitions to the $2p_{3/2}$, $2p_{1/2}$, and $1f_{5/2}$ states, the angular distribution of transitions to the weakly excited states display the forward-peaked oscillatory features characteristic of the direct transfer process. Therefore the usual distorted-wave Born-approximation (DWBA) formalism has been applied to extract l values and spectroscopic factors. Unfortunately the DW treatments use different optical potentials; moreover, there are serious discrep-

ancies in the published values of the absolute cross sections. In addition, the parameter values extracted from certain of the angular distributions are ambiguous. In the present work new measurements on the weak transitions at 9 and 20 MeV deuteron energy are presented, together with additional data on the stronger transitions acquired at $E_d = 13$, 16, and 19.3 MeV. A simple optical model is used to analyze all the data available from $E_d = 7$ to 20 MeV. The results confirm certain of the ^{49}Ca assignments suggested in Ref. 5 and modify others.

The forward-peaked oscillatory angular distributions observed suggest that the standard one-step DWBA formalism may be adequate, even though it is known[12] that weak transitions to fragments far from the centroids of the single-particle strength are poorly represented by conventional single-particle form factors. Inasmuch as this formalism provides an acceptable representation of many of the measured angular distributions, we have concluded that higher-order reaction contributions, *in these instances*, are not large. There remain, however, certain "anomalous" angular distributions which cannot be reproduced by the standard formalism. Therefore, the analyses presented herein are considered interim, pending a more complete treatment possible via coupled-channel techniques that also include a more sophisticated modeling of the nuclear structure involved.

Crucial to any DWBA analysis is the assumption that resonances do not affect either the incoming or the outgoing channels. Brown *et al.*[11] have concluded that compound nuclear effects in the ^{48}Ca-(d,p) reaction are small in the range $7 < E_d < 10$ MeV, although the possibility of significant interferences between direct and compound nuclear processes was not explored. We believe that a straightforward demonstration that interference from compound nuclear effects can be neglected safely is afforded by a careful study of the energy dependence of the yields. Accordingly, at two angles the yields of elastically scattered deuterons and of protons to the well-known $2p_{3/2}$ and $2p_{1/2}$ single-particle states were measured from 6 to 20 MeV deuteron energy. These data, supplemented by the measurements of Bogaards and Roy[9] from 2 to 5.5 MeV deuteron energy show, by their smooth energy variation, that no significant resonance effects with widths greater than 200 keV are present in the strong transitions. However, we did not obtain such data for the forbidden transitions.

After a description of the experimental arrangements, Sec. II of this paper presents the analysis of the measured proton energy spectra, and iden-

tifies several ^{49}Ca states not observed previously. Section III is devoted to the deuteron elastic scattering data and to the study of the protons populating both $2p$ states and the $1f_{5/2}$ state in ^{49}Ca. From these and other data, the parameters used in the subsequent DWBA analyses are extracted. Section IV presents the data and the analyses of the remaining proton angular distributions observed.

The γ-ray decays of certain of the ^{49}Ca levels have been studied by Canada, Ellegaard, and Barnes.[5] Their measurements of branching ratios, together with the angular momentum transfer established in Ref. 1 and in the preliminary report of the present work,[13] were used to limit the spins of certain states and to permit comparison of the observed level scheme with predictions of a core-coupling model. Their suggestions are discussed in Sec. V.

II. EXPERIMENTAL ARRANGEMENTS AND ENERGY SPECTRUM

The present data were obtained using the Wright Laboratory MP tandem Van de Graaff accelerator to furnish deuteron beams up to 20 MeV energy, and a multigap magnetic spectrograph to measure the outgoing charged particles. The charged particles were detected in nuclear emulsions placed in the focal surfaces of the 23 spectrograph gaps. The nominal shape of the calibration curve (the relation between position along the focal surfaces and radius of curvature) was determined by elastic scattering measurements. The energy calibration was determined using particle groups from reactions of known Q values. Energy resolution is determined by the energy spread of the incident beam, the target thickness, and the dimension of the beam-illuminated spot on the target. In the present experiment $E/\Delta E$ was approximately 1500, corresponding to an over-all proton energy spread of 15 keV. Details of the instrument, its adjustment, and its calibration are available in Ref. 14.

Targets for these experiments were prepared by evaporating a layer (~60 μg/cm^2) of metallic ^{48}Ca (enrichment 98.3%, supplied by the Oak Ridge National Laboratory) onto 40 μg/cm^2 carbon foils strengthened by a 5 μg/cm^2 layer of Formvar fore and aft. Contaminant nuclei in these targets (determined from kinematic shifts in the momenta of their reaction products) were H, ^{12}C, ^{13}C, ^{14}N, ^{16}O, ^{18}O, ^{28}Si, and ^{40}Ca. Carbon was especially bothersome because the ^{12}C$(d,p)^{13}$C yields to the 3.09 and 3.86 MeV states of ^{13}C obscured ^{49}Ca states from 4.3–4.9 MeV excitation at many angles forward of 50°. A thicker (2.1 mg/cm^2) self-supporting ^{48}Ca foil was used in a conventional

76.2 cm Ortec scattering chamber to obtain the excitation functions described in Sec. III.

Because the identification of individual tracks in nuclear emulsions becomes inaccurate if a critical track density is exceeded, our spectrograph data fall into two classes, namely short exposures used to study the strong transitions and long exposures designed to study the weak transitions. Figure 1 shows a "long exposure" spectrum; here the weakly excited transitions are clearly visible. For the proton data, plate scanning was simplified by placing over the emulsion Al foils of thickness sufficient to stop the deuterons. In extracting relative cross sections, the areas of complex peaks were resolved by the peak-fitting program AUTOFIT.[15] However, some ^{49}Ca peaks were overlapped by the shoulders of the very intense peaks associated with C and O con-

taminants; in such cases a background simulating the shoulder was subtracted from the peak of interest, and the error in the extracted cross section was increased appropriately. Relative cross sections from different spectrograph exposures were established by use of a monitor detector and a beam current integrator. Absolute cross sections were taken from the yield measurement described in Sec. III.

In all, 25 states in ^{49}Ca were observed in the present experiment. Their excitation energies are given in Table I, together with the corresponding energies as determined in previous experiments. (It should be noted that the present excitation energies are derived from observed differences in plate distance and a calibration slightly adjusted with an effective field calculation to maintain a ground-state Q value of 2.924 MeV in all
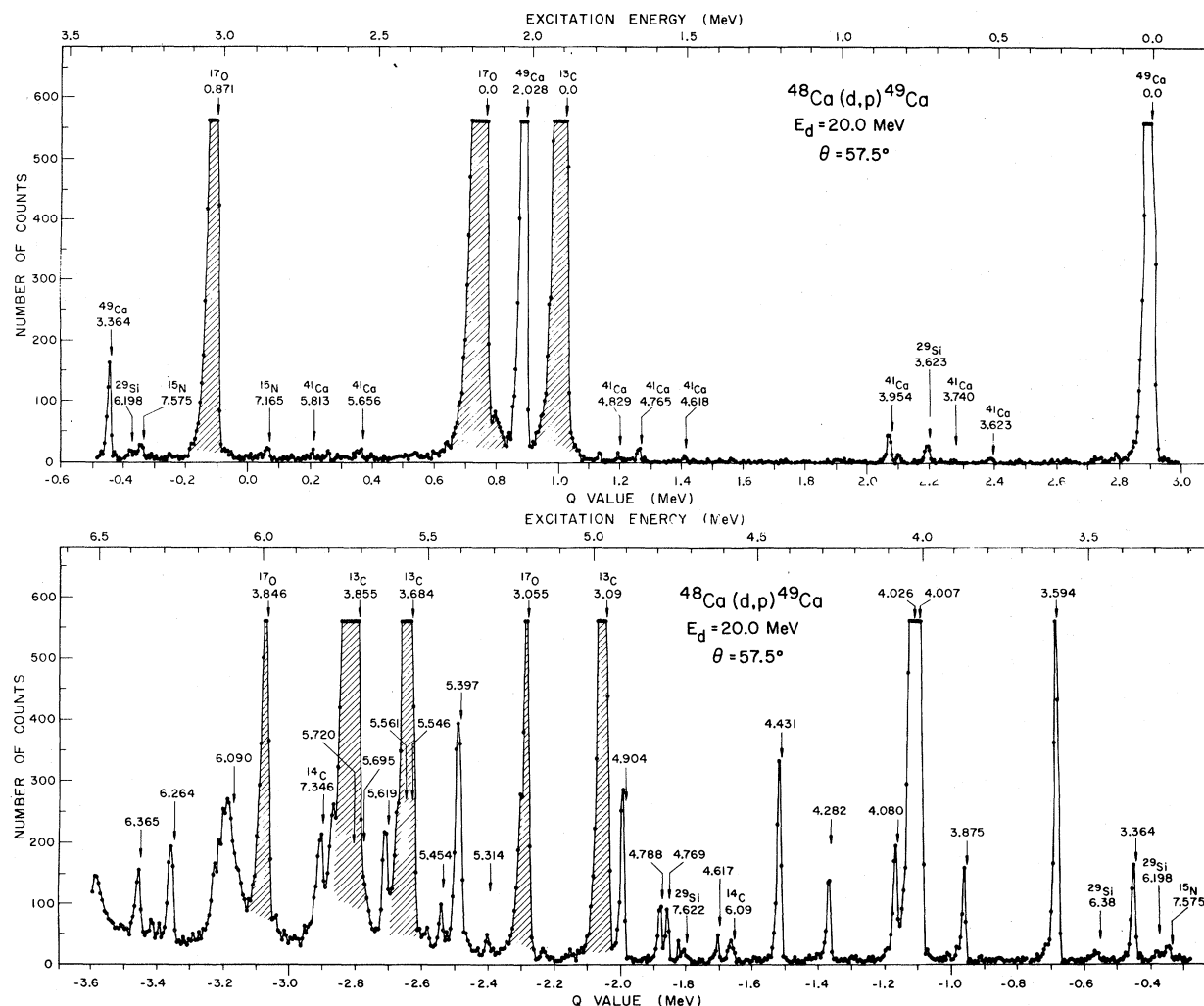

FIG. 1. Typical proton spectrum measured in the magnetic spectrograph.

TABLE I. Excitation energies for states of ^{49}Ca (energies in MeV, errors in keV).

This work		Kashy et al.[a]		Erskine et al.[b]		Canada et al.[c]	
g.s.		g.s.		g.s.		g.s.	
2.028	5	2.028	4	2.027	4	2.022	2
3.364[d]	6	3.371	7	3.357	4	3.351	2
3.594	5	3.595	7	3.589	4	3.586	2
3.875[d]	5					3.861	2
4.007	6	4.005	8	4.001	4	3.991	2
4.026	6	4.024	8	4.020	7	4.010	3
4.080[d]	6	4.078	8	4.078	10	4.065	2
4.282[d]	6	4.279	10	4.278	10	4.272	2
4.431	6	4.422	9	4.423	10	4.416	2
4.617[d]	6						
4.769[d]	6						
4.788[d]	6						
4.904[d]	6					4.885	3
5.314[d]	6						
5.397[d]	6	5.387	10	5.394	5		
5.454[d]	10						
5.546[d]	8						
5.561[d]	8						
5.619[d]	7						
5.695[d]	9						
5.720[d]	9						
6.090	15	6.095	15				
6.264[d]	12						
6.365[d]	12						

[a] ^{48}Ca$(d,p)^{49}$Ca, MIT magnetic spectrograph, Ref. 1.
[b] ^{48}Ca$(d,p)^{49}$Ca, ANL magnetic spectrograph, Ref. 2.
[c] ^{48}Ca$(d,p\gamma)^{49}$Ca, Ge(Li) detector, Ref. 5.
[d] Excitation energy measured with respect to the level at 3.594 MeV.

gaps.) The results are generally in good agreement with earlier measurements, the largest discrepancy being the 20 keV variation in the energy of the state here denoted 3.364 MeV in excitation.

III. DETERMINATION OF THE OPTICAL POTENTIALS

In this section, l values and spectroscopic factors are assigned on the basis of standard DW analyses. First, to check the applicability of the direct reaction mechanism, the yields of the elastic deuteron scattering and the protons to the $2p_{3/2}$ and $2p_{1/2}$ states were measured in 200 keV steps over the full range of deuteron energy accessible, using solid state detectors in a conventional scattering chamber. Although the data were acquired in several distinct runs, the deuterons scattered from hydrogen in the target afforded a very convenient internal normalization. The elastic scattering data are shown in Fig. 2 together with the prediction calculated by code ABACUS[16] using deuteron parameters which best fitted the 19.3 MeV data.[17] The data join smoothly with those of Bogaards and Roy,[9] and are well fitted, particularly at the more forward angles, by the optical model

with fixed parameters. Since the target used for this experiment was about 50 keV thick, it was conceivable that it averaged over closely spaced compound nuclear resonances; therefore the insert shows data measured with the 10 keV target used in the high resolution spectrograph exposures. These data are taken as evidence that compound nucleus resonances are not affecting the data. The 50° point at 2 MeV (consistent with data from other angles from 40–80° at the same energy) was used to establish the scale of absolute cross section for the entire experiment by assuming that pure Rutherford scattering obtained. Figures 3 and 4 illustrate the energy dependence of the (d, p) yields to the $2p_{3/2}$ and $2p_{1/2}$ states over the same deuteron energy range. Again, there is no evidence of resonance or fluctuation phenomena. The predictions of the energy dependence of the DW cross section for these two states (assuming $S = 1$) are taken from calculations with code DWUCK.[18] From the smooth energy dependence of the three cross sections measured over the broad energy range 2 to 20 MeV, it is concluded that the direct mechanism dominates the reaction. Though the (d, d_0) points at $E_d \sim 9$ MeV, $\theta = 120°$ are lower than

the fixed-parameter prediction, we believe that the DW process satisfactorily accounts for all the gross features of the observed energy dependence.

Having established, by the absence of obvious resonances, that a simple DW treatment may apply to the single-particle states, we chose for the optical model for both protons and deuterons a standard Woods-Saxon form. The potential is the sum of a real, an imaginary (surface absorption), a spin-orbit, and a Coulomb term: real term $= -V_0 f(r, r_{0R}, a_{0R})$; surface absorption term $= i \, 4 a_{0I} W_D (r/dr) f(r, r_{0I}, a_{0I})$; spin-orbit term $= (\lambda V_0 / 45.2)(1/r)(r/dr) f(r, r_{0R}, a_{0R})(\vec{l} \cdot \vec{s})$; Coulomb term $= (Ze^2/2R_C)(3 - r^2/R_C^2)$, $r \leq R_C$, Ze^2/r, $r > R_C$; $f(r, r_0, a_0) = 1/[1 + \exp(x)]$, $x = (r - r_0 A^{1/3})/a_0$; $R_C = r_{0C} A^{1/3}$. All potential depths in MeV; all lengths in femtometers. Although the results are not very sensitive to the choice of the proton potential, the particular proton parameters used were those of Peterson,[19] derived from a study of proton scat-

tering from ^{48}Ca at 17.5 MeV. They are: $V_0 = 42.9$, $r_{0R} = 1.34$, $a_{0R} = 0.76$, $W_D = 16.0$, $r_{0I} = 1.25$, $a_{0I} = 0.05$, $\lambda = 32$, $r_{0C} = 1.25$. For the deuteron potential it was decided to set the spin-orbit term equal to zero, because previous analyses[20] have shown that unless deuteron polarization data are available, no consistent spin-orbit terms can be extracted. The Coulomb radius was set at $r_{0C} = 1.30$, leaving six deuteron parameters available to fit the elastic scattering and (d, p) data. We attempted to constrain these by requiring the theory to fit, as well as possible, all the data available within the range 7 MeV $\leq E_d \leq 20$ MeV, namely: (a) the 13.0, 16.0, and 19.3 MeV deuteron elastic scattering differential cross sections shown in Fig. 5; (b) the (d, p) cross sections populating the single-particle states, measured at the same energies, shown in Fig. 6; (c) the 7.0–7.5 MeV elastic scattering data and the (d, p) angular distributions to the single-particle states, reported in
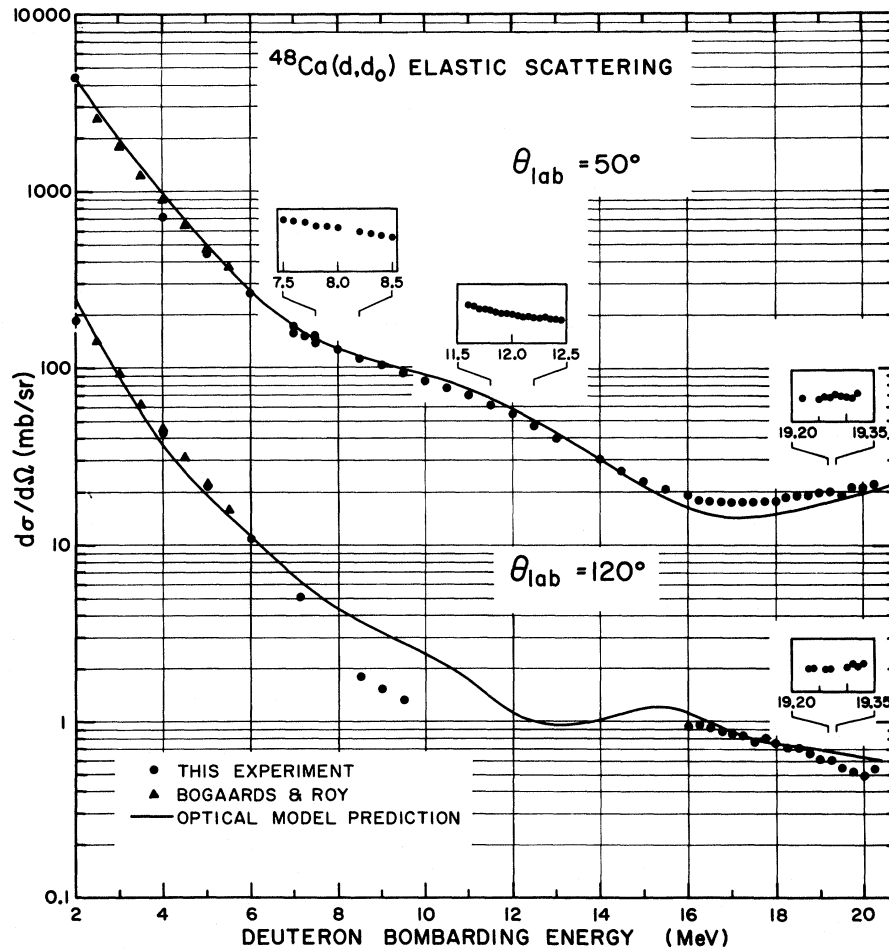

FIG. 2. Yield of deuterons elastically scattered from ^{48}Ca. The solid line is an optical-model prediction.
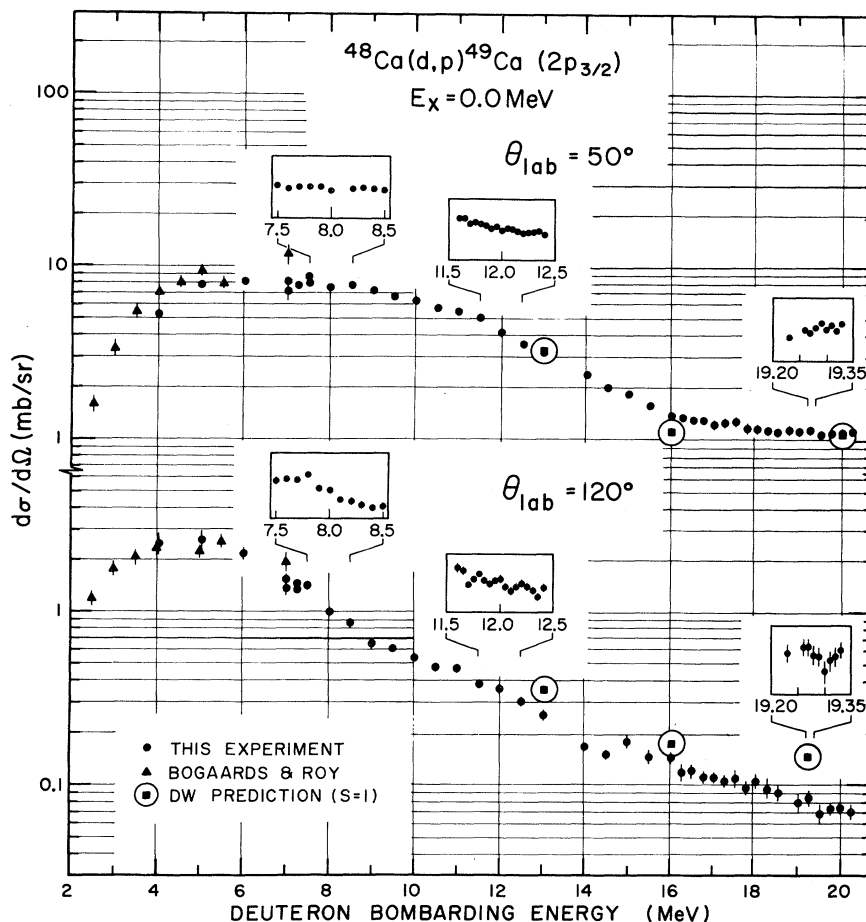
FIG. 3. Yield of protons populating the $2p_{3/2}$ ground state of ^{49}Ca. The encircled squares are theoretical DWBA predictions, assuming the spectroscopic factor to be one.

Refs. 1 and 6; (d) the 9–12 MeV elastic scattering data of Ref. 21; (e) the 10 MeV elastic scattering data and the (d, p) angular distributions to the single-particle states reported in Refs. 7, 8, and 11.

Unfortunately, some of these data, as reported, are in substantial conflict; to obtain consistence, arbitrary decisions were necessary. First, the 10 MeV elastic scattering data of Ref. 21 disagrees with the more recent measurements of Ref. 8; we have chosen to ignore the data of Ref. 21. Second, the absolute (d, p) cross sections cited in Ref. 1 for populating the ground state disagree with more recent measurements from the same laboratory reported in Ref. 6. We accept the absolute cross sections of Ref. 6; accordingly, all the (d, p) cross sections of Ref. 1 have been renormalized by multiplying them by 0.55. Third, at $E_d = 10$ MeV the absolute (d, p) cross sections for populating the ground state cited in Refs. 8 and 11 disagree with that reported in Ref. 7. Because Refs. 6 and 7 used the same target, on

grounds of consistence we have renormalized the absolute cross sections of Refs. 8 and 11 to those of Ref. 7 by multiplying them by 1.22.

From a search described in detail in Ref. 17 the geometric parameters of the deuteron potential were fixed at the values $r_{0R} = 0.972$ fm, $a_{0R} = 0.892$ fm, $r_{0I} = 1.414$ fm, $a_{0I} = 0.655$ fm, and the problem was reduced to finding appropriate values of the deuteron well depths V_0 and W_D. From consideration of the parameter searches cited in Refs. 6, 7, and 8 it became clear that we could not hope to find satisfactory constant values of V_0 and W_D. We therefore tried simple energy dependencies similar to those used by Schwandt and Haeberli.[20] For W_D, values of 13 MeV for 7 MeV $\leqslant E_d \leqslant 13$ MeV, 16 MeV for $E_d = 16.0$ MeV and 21 MeV at 19.3 MeV were used, presumably reflecting the increase in the number of outgoing channels as the deuteron energy increases. (The results were not very sensitive to the specific values.) For V_0, a simple relation of the form $-V_0 = 127 - 0.7$ E_d (MeV) was chosen. The form of the energy
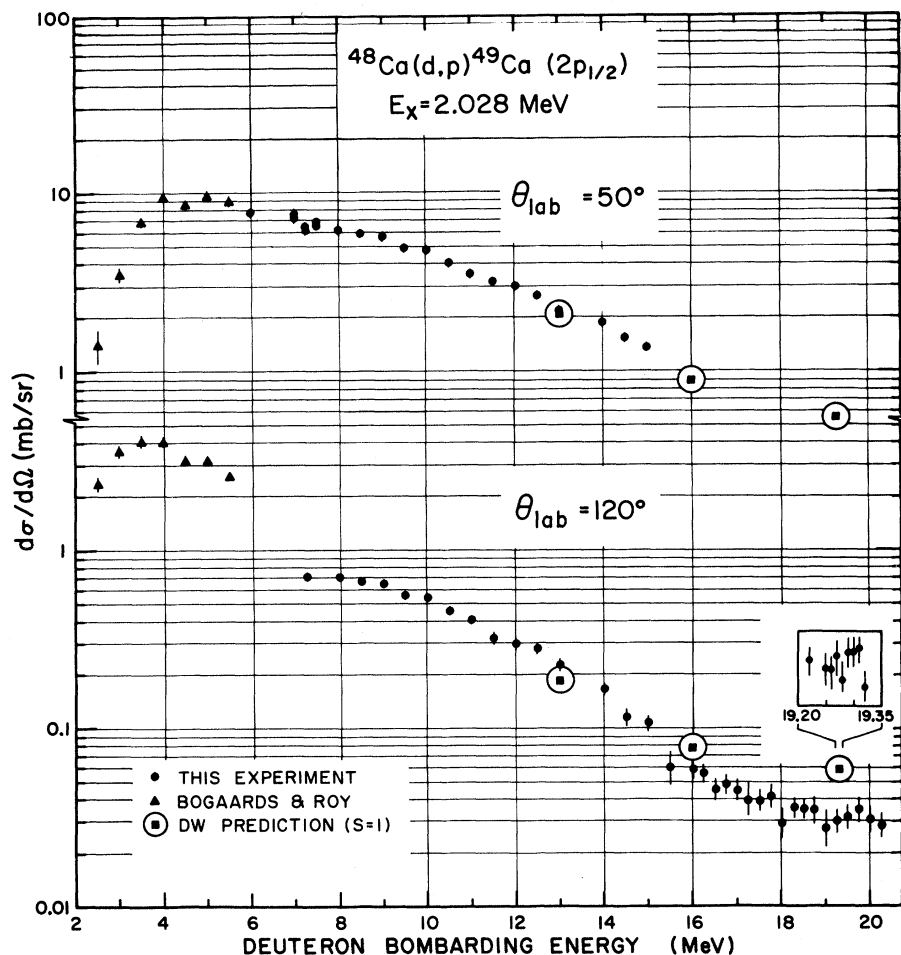
FIG. 4. Yields of protons populating the $2p_{1/2}$ single-particle state of ^{49}Ca. The encircled squares are theoretical DWBA predictions, assuming the spectroscopic factor to be one.

dependence is that suggested by Perey and Perey[22] to compensate for nonlocality effects, though the coefficient of E_d is larger than the one they recommend. The resulting deuteron potential is referred to as the AV GEOM potential henceforth. At the corresponding energy it is quite similar to the CA46 potential used in Refs. 6 and 7, and is related through the $V_0 r_{0R}^n$ degeneracy to that used in Refs. 8 and 11.

For the neutron form factors the conventional well-depth method was used. The form of this well was again the familiar Woods-Saxon shape with the geometrical parameters r_0 and a_0 chosen to be 1.25 fm and 0.65 fm. The spin-orbit strength $\lambda = 25$ reproduces the $2p_{3/2}$-$2p_{1/2}$ level splitting in ^{49}Ca.

The predictions resulting from inserting these choices of proton, deuteron, and neutron parameters into code DWUCK[18] are shown as solid lines in Figs. 5 and 6. It is obvious that our parameter searches sought to emphasize the fits at for-

ward angles, where direct reactions are expected to dominate. It is also clear that better fits to the deuteron elastic scattering could be obtained by searching for best fits at each of the three energies. However, our "best fits" to the deuteron scattering at each energy did not display the systematic variations of parameters consonant with the spirit of the optical model; further, the fits to the (d, p) single-particle transitions are improved by using the AV GEOM rather than the "best fit" parameters.[17] Our parameters also provide fits to the renormalized 10 MeV data that are as good as those cited in Ref. 11. For the renormalized 7.0–7.5 MeV (d, p) angular distributions, the fits are respectable, though not always quite as good as those achieved in Ref. 1; the worst fit is to the 7.0 MeV elastic deuteron scattering, for which the AV GEOM potential predicts cross sections for $\theta > 90°$ that are only 60% of the observed[6] cross section. For the (d, p) reaction it is important to note that not only the angular
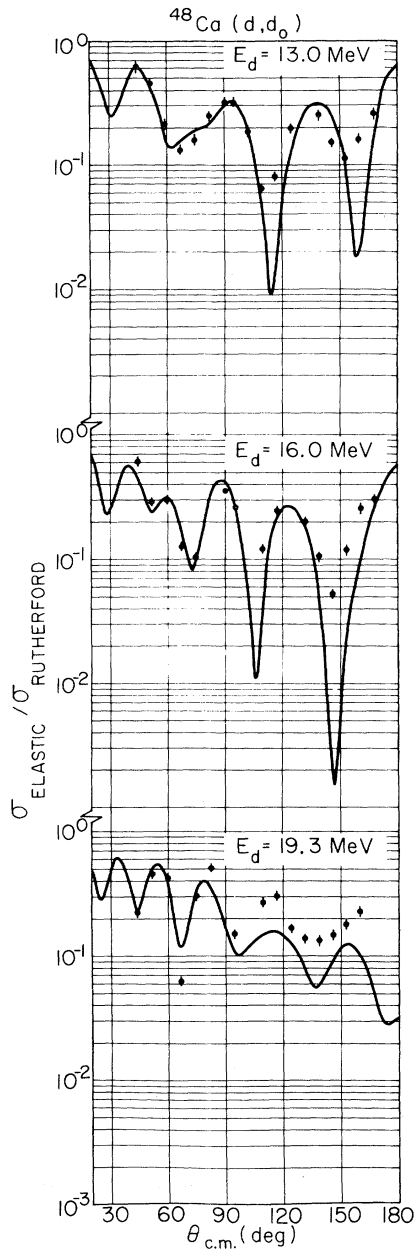
FIG. 5. Angular distributions of elastically scattered deuterons obtained with the magnetic spectrograph. The solid lines are optical-model predictions using the AV GEOM parameters described in the text.

distributions, but also the absolute cross sections for the allowed transitions and their energy dependencies, are well predicted. The latter are shown in Table II, a list of spectroscopic factors derived from the DWBA fits. For pure single-particle transitions $S = 1$ necessarily, and only ~10% deviations from this value are found for the $2p_{3/2}$ and $2p_{1/2}$ transitions. Considering the neglect of nonlocal effects in the proton potential, of

deuteron-breakup effects in the deuteron potential, and of finite-range and spin-orbit effects in both proton and deuteron potentials, the values in Table II for allowed transitions are remarkably good. The $1f_{5/2}$ state is known to be fragmented; the portion of single-particle strength missing from the 4.007 MeV level appears to reside in the 3.594 MeV state discussed subsequently.

IV. THE FORBIDDEN TRANSITIONS

In addition to the three strong single-particle transitions discussed in Sec. III, less intense proton groups populating 11 states below 5 MeV excitation (see Table I) were clearly observed at 11 or more angles. These are the "forbidden transitions." Comprehensive angular distributions were obtained for all of these with the exception of that to the 4.617 MeV state. As noted in Sec. I, the variation in intensity of the proton groups required that different spectrograph exposures be utilized to cover the cross-section range encountered. The bulk of the data for the forbidden transitions was obtained from the long exposures at $E_d = 20$ MeV, but note that some of our angular distributions contain data taken at 19.3 MeV as well as at 20 MeV. These data, however, join smoothly and have not been adjusted to compensate for this slight difference in incident energy. (DWBA calculations using the parameters described in Sec. III indicate that the energy-dependent differences are expected to be within the experimental errors of the data.) For the forbidden transitions, the data at 19.3–20 MeV constitute the primary source. However, for certain of these transitions, an initial analysis yielded results not consistent with the 7.5 MeV MIT data.[1] Therefore, for some of the states, new partial angular distributions were obtained at 9 MeV, this energy being chosen to minimize interference from troublesome contaminant groups originating from ^{12}C in the target. Even so, contaminant interference limits the accuracy and angular range of our 9 MeV data.

In the following the transitions are discussed individually. In each case, DW curves calculated using code DWUCK[18] with the AV GEOM optical model parameters discussed in Sec. III are shown, together with an indication of the single-particle form factor used and the spectroscopic factor S. The well depths with which the single-particle form factors were calculated were adjusted so that the separation energy matched that of the state in question. Spectroscopic factors S were obtained as the factor required to normalize the calculated curves to the experimental angular distributions; for an idealized single-particle level, $S = 1$. Table II lists the spectroscopic fac-
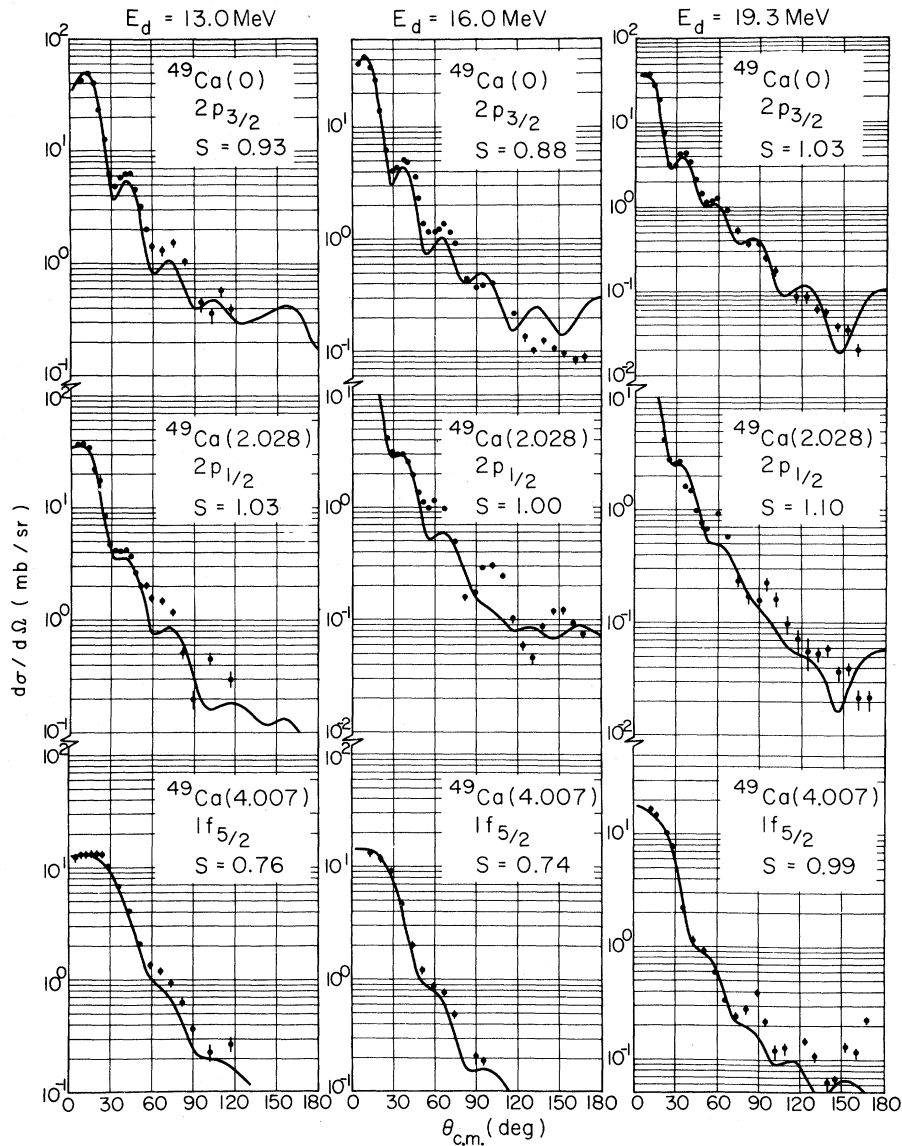
FIG. 6. Angular distributions of protons populating the single-particle states of ^{49}Ca. The solid lines are DWBA fits using the AV GEOM parameters.

tors obtained not only for the present data, but also for the renormalized data of Refs. 1 and 11. When the fits of the curves to the first maximum of the data are somewhat poorer than desired, the corresponding spectroscopic factor in Table II is enclosed in parentheses: such values are not included in the tabulated averages. For some transitions a consistent assignment of l and S is not possible; these transitions are termed anomalous, and are discussed later in this section.

A. $l=1$ transition: 4.080 MeV state

In the 7.5 MeV experiment of Ref. 1, data for this state were obtained only for angles greater

than 30°; these data being similar to those for the strong $l=3$ transition to the 4.007 MeV state, the 4.080 MeV level was assigned $l=3$ in Ref. 1. However, the more complete data now available does not permit an unambiguous assignment unless both the energy and the angular dependencies are considered. In the 9 MeV data of the present experiment the forward point (at 12.5°) is significantly higher than the 25° point, contrary to the $l=3$ prediction. This rise suggests the possibility of an $l=1$ assignment although, as Fig. 7 shows, the forward point is too low to offer convincing support for that hypothesis. At 20 MeV, Fig. 7 shows that $l=1$ follows the trend of the data better than

TABLE II. Spectroscopic factors.

E_{ex} (MeV)	$\psi_{s.p.}$	7.0 [a]	7.5 [a]	9.0 [b]	10.0 [c]	13.0 [b]	16.0 [b]	19.3 or 20.0 [b]	Av.
					E_d (MeV)				

		Allowed transitions							
0	$2p_{3/2}$	0.92	⋯	⋯	0.88	0.93	0.88	1.03	0.93
2.028	$2p_{1/2}$	0.87	⋯	⋯	0.92	1.03	1.00	1.10	0.98
4.007	$1f_{5/2}$	⋯	0.87	0.71	0.70	0.76	0.74	0.99	0.80

		Forbidden transitions							
3.364	$2d_{5/2}$	⋯	0.0061	0.0041	(0.0043)	⋯	⋯	d ⎫	anomalous
	$1g_{9/2}$	⋯	d	d	d	⋯	⋯	0.018 ⎭	
3.594	$1f_{5/2}$	0.15	0.15	0.12	0.13	⋯	⋯	0.17	0.14
3.875	$2p_{3/2}$	⋯	⋯	0.0021	d	⋯	⋯	d ⎫	anomalous
	$1g_{9/2}$	⋯	⋯	d	e	⋯	⋯	0.010 ⎭	
4.026	$1g_{9/2}$	⋯	0.27	f	g	0.27	0.27	0.37	0.30
4.080	$2p_{3/2}$	⋯	0.024	0.023	0.024	⋯	⋯	0.020	0.023
	$1f_{5/2}$	⋯	0.067	0.050	(0.035)	⋯	⋯	0.024	Not consistent
4.282	$2d_{3/2}$	⋯	h	0.023	0.013	⋯	⋯	0.021	0.019
4.431	$2d_{5/2}$	⋯	0.035	0.029	i	⋯	⋯	0.047	0.037
4.788	$1g_{9/2}$	⋯	⋯	⋯	⋯	⋯	⋯	(0.0053)	⋯
4.904	$1g_{9/2}$	⋯	⋯	j	(0.020)	⋯	⋯	(0.021)	⋯

[a] Ground state, Ref. 6; other states, Ref. 1, renormalized to Ref. 6.
[b] Present measurement.
[c] Reference 11, renormalized to Ref. 7.
[d] DWBA calculation does not resemble data.
[e] DWBA curve not a good fit, but compatible with $S=0.016$.
[f] Data of marginal quality, but consistent with $S=0.26$.
[g] DWBA curve not a good fit, but compatible with $S=0.27$.
[h] DWBA curve does not fit data unless data at $\theta < 30°$ is ignored; if so, $S=0.025$.
[i] Except for two forward angle data points, good fit with $S=0.031$.
[j] Data of marginal quality, but compatible with $S=0.017$.

$l=3$; however, the patterns $l=1$, 2, and 3 are not very distinct from one another. In the 10 MeV data of Ref. 11, the $l=1$ curve fits somewhat better than the $l=3$ prediction, but no data exist for $\theta < 25°$, the region in which $l=1$ and $l=3$ differ distinctively. Thus, for this transition, the angular distributions taken separately do not offer a clear choice between $l=1$ and $l=3$. However, the DWBA prediction of the energy dependence of the yield between 7.5 and 20 MeV for these l values is quite different. Table II shows that an $l=3$ assignment implies a decrease in S of a factor of 2.8 over that range, whereas an $l=1$ assignment yields a consistent value for S at each of the four energies at which data are available. We believe this to be convincing evidence that the state is populated by an $l=1$ transition. The γ ray corresponding to decay to the $\frac{3}{2}^-$ ground state was observed by Canada et al.[5]; no transitions to other states were seen. The identification of the 4.080 MeV state as $\frac{7}{2}^-$, favored by the authors of Ref. 5, is a direct consequence of the $l=3$ assignment of Ref. 1, and cannot be considered firm in the light of the present data. The γ-decay data are not in-

consistent with a spin-parity of $\frac{1}{2}^-$ or $\frac{3}{2}^-$, as implied by the present $l=1$ assignment.

B. $l=2$ transitions: 4.282 and 4.431 MeV states

At 20 MeV deuteron energy, the over-all shape of the DW curves is nearly the same for $l=2$ transfer as for $l=1$ transfer at ~4 MeV excitation energy; however, the predicted minima for the $l=2$ curves are more pronounced and occur at larger angles. Though an $l=1$ assignment is conceivable, at 20 MeV, on the basis of the quality of the fit of the $l=2$ DW curves to the structure of the angular distributions between 20° and 120° shown in Fig. 8, an $l=2$ assignment is clearly preferred for both states. At 9 MeV, again $l=2$ provides an excellent fit for both states though the data is limited in angular range. The $l=2$ assignment agrees with that of Kashy et al.[1] for the 4.431 MeV state; although these authors observed the 4.282 MeV level, their angular distribution information was insufficient to justify an l assignment for this transition. In fact, an $l=2$ assignment for the 4.282 MeV level is compatible with their data only if the more forward point (30°) is ignored (see Fig. 8). Turning
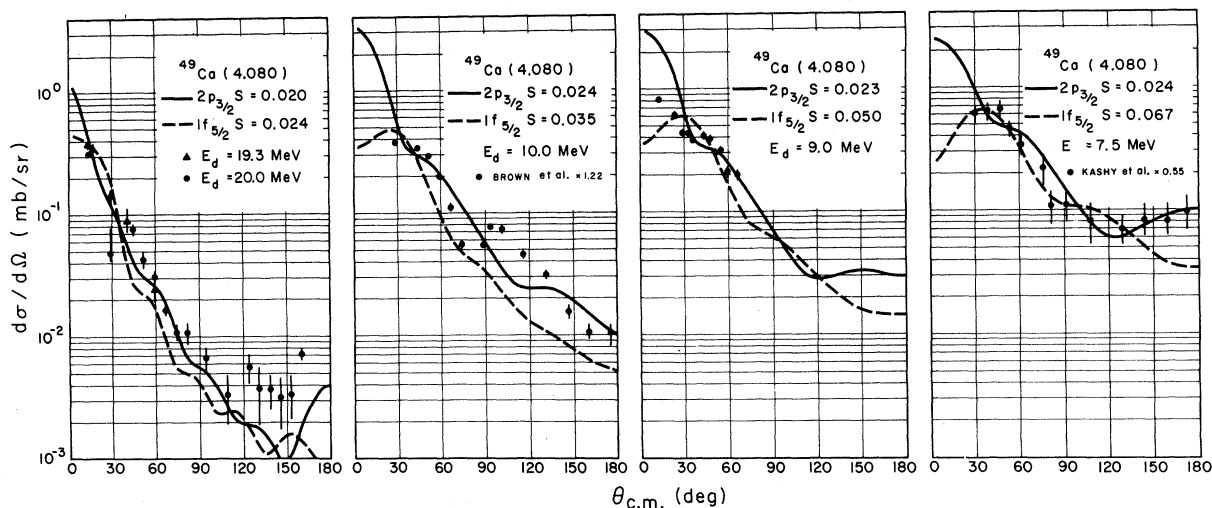
FIG. 7. Angular distributions of protons populating the 4.080 MeV state in ^{49}Ca. The data at 7.5 and 10 MeV are taken from Refs. 1 and 11, renormalized as indicated. The data at 9 and 19.3 + 20 MeV are from the present measurement. The curves are the DWBA predictions using the AV GEOM parameters, with spectroscopic factors as indicated. The solid lines represent the preferred assignment.

to the 10 MeV data, Brown et al.[11] do not make an l assignment to the 4.282 MeV state. However, our $l = 2$ prediction is quite compatible with their renormalized data. For the transition populating the 4.431 MeV level, our $l = 2$ prediction is compatible only if the two most forward points are ignored; however, the authors of Ref. 11 also make the $l = 2$ assignment, though the same difficulty obtains with their prediction. Table II shows a wider fluctuation in S than is usual, but no trend with energy exists. We conclude that the $l = 2$ assignment is acceptable for both states.

At 20 MeV, the 4.282 MeV transition exhibits a rise at ~135° which the 4.431 MeV transition does not; this may be a j-dependent effect. In the ^{32}S-(p, d) reaction the $d_{3/2}$ transition has been observed[23] to have a more pronounced angular distribution than the $d_{5/2}$ transfer, suggesting a $d_{3/2}$ assignment to the 4.282 MeV level and a $d_{5/2}$ assignment to the 4.431 MeV state.

Canada et al.[5] have assigned a spin of $\frac{1}{2}$ or $\frac{3}{2}$ to the 4.282 MeV state on the basis of the strength of the γ decay to the 2.028 MeV $\frac{1}{2}^-$ state. The present assignment of $l = 2$ fixes the level as $\frac{3}{2}^+$. For the 4.431 MeV level, the $l = 2$ assignment is consistent with either a $\frac{3}{2}^+$ or $\frac{5}{2}^+$ assignment. Canada et al. prefer the $\frac{5}{2}^+$ value because of the absence of a competing $E1$ branch to the 2.028 MeV $\frac{1}{2}^-$ state.

C. $l = 3$ transition: 3.594 MeV state

At $E_d = 20$ MeV, the angular distribution of the transition to the state at 3.594 MeV shown in Fig. 9 is nearly identical to that for the strong $l = 3$

transition to the 4.007 MeV level (Fig. 6). Both sets of data show a clear secondary maximum at ~85° and differ very little even at backward angles. In each case the DW curve predicts the distribution very well at angles up to the secondary maximum, but is somewhat low at angles further backward. The partial angular distribution obtained at 9 MeV is well fitted by $l = 3$ at forward angles. The $l = 3$ prediction also fits the 7.5[1] and the 10 MeV[11] data, and Table II shows the spectroscopic factors at all energies to be consistent. This transition clearly displays the characteristics of $l = 3$ transfer. The DW predictions for $1f_{5/2}$ and $1f_{7/2}$ transitions differ only minutely from one another, so fail to yield any basis for a choice of the j assignment. Because of the predicted shell-model level ordering for ^{48}Ca—namely that the $1f_{7/2}$ orbital is filled by the 28th neutron of ^{48}Ca and the $1f_{5/2}$ is empty—the $1f_{5/2}$ assignment is made. This interpretation agrees with the conclusions of Kashy et al.,[1] and is further reinforced by the data of Canada et al.[5] The average value of the spectroscopic factor for the 3.594 MeV state is 0.14 (see Table II), while that for the 4.007 MeV level is 0.80. It appears that the single-particle $1f_{5/2}$ strength is split between the two levels, so that the center of gravity of the $1f_{5/2}$ strength lies at 3.946 MeV in ^{49}Ca.

D. $l = 4$ transition: 4.026 MeV state

Figure 10 shows that a DW $l = 4$ curve predicts the angular dependence of the transition populating the 4.026 MeV level very well at 19.3 MeV, and reasonably well at 16.0 and 13.0 MeV. At 9 MeV (as at 10 MeV) the data at forward angles appear
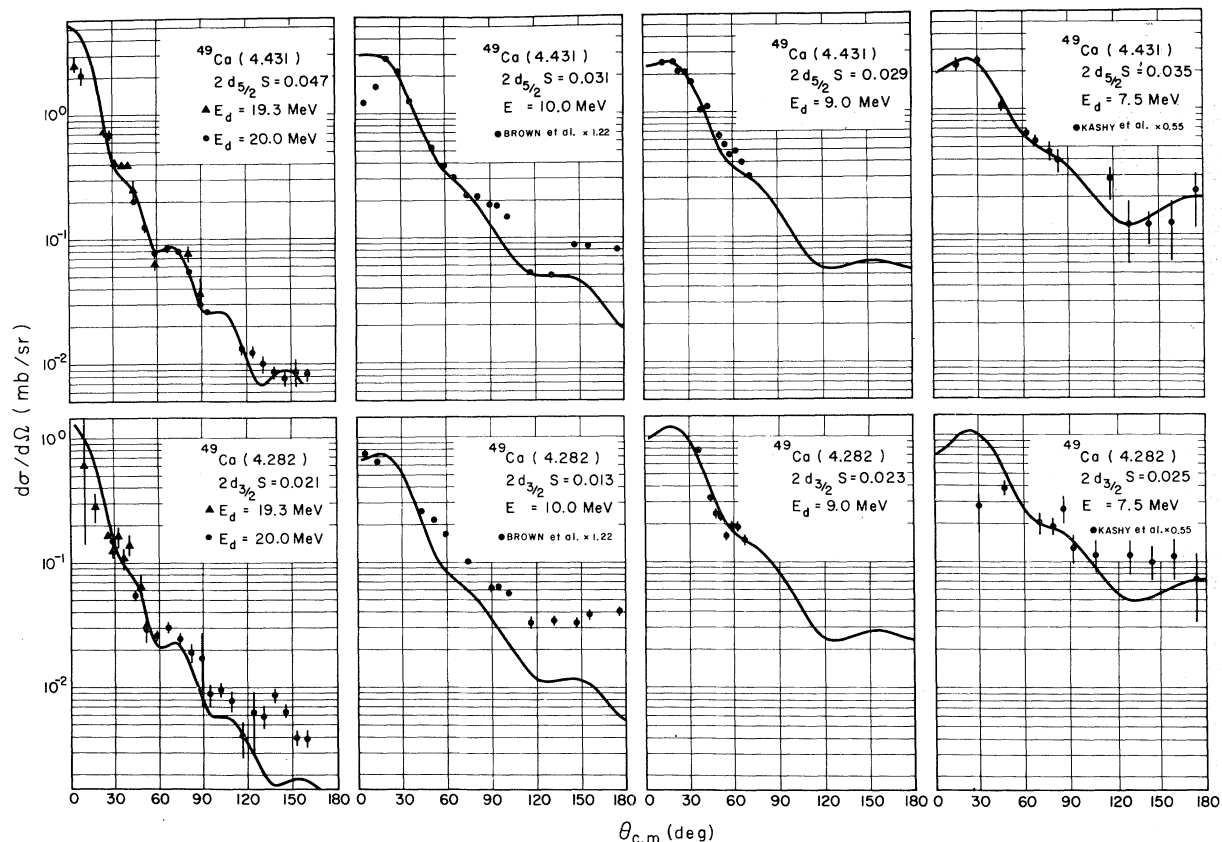
FIG. 8. Angular distributions of protons populating the 4.282 and the 4.431 MeV states. The data at 7.5 and 10 MeV are taken from Refs. 1 and 11, renormalized as indicated. The data at 9 and 19.3+20 MeV are from the present measurement. The solid curves represent the DWBA predictions using AV GEOM parameters, with spectroscopic factors as indicated. The choice of j is justified in the text.

to increase slightly, contrary to the DWBA prediction. Nevertheless, this state clearly represents a significant fraction of the $l = 4$ strength. The spectroscopic factors listed in Table II are reasonably consistent, although the value at 19.3 MeV is rather high. On the basis of the large $\vec{l} \cdot \vec{s}$ splitting of the $g_{9/2}$-$g_{7/2}$ strength expected, the transition is treated in Table II as $1g_{9/2}$ in agreement with the conclusion of Kashy et al.[1] However, $1g_{7/2}$ DW curves differ from $1g_{9/2}$ curves only in over-all magnitude. Since the $1g_{9/2}$ single-particle state is expected at about 5.9 MeV excitation,[24] it is interesting to speculate about the interaction responsible for the 1.9 MeV shift. We shall return to this point in Sec. V.

E. Anomalous transitions: 3.364 and 3.875 MeV states

For the levels cited, the angular distributions shown in Fig. 11 display the forward-peaked oscillatory signature of direct interaction, but the best fits available within the DWBA model are not of a quality comparable to those described above.

Further, in these cases neither the angular distribution or the yields as a function of incident energies are consistent with assignment of a unique l.

1. 3.364 MeV level

The earlier study of this transition,[1] obtained at 7.5 MeV deuteron energy, resulted in an $l = 2$ assignment (and would again, even with the present DWBA parameters). The 9 MeV data, though limited, are consistent with the earlier data; were these the only data available, an $l = 2$ assignment would be reasonable. However, the 20 MeV data, also shown in Fig. 11, are clearly inconsistent with $l = 2$ at forward angles; at this energy an $l = 4$ assignment might be preferred to any other. However, at larger angles the observed cross sections exceed the $l = 4$ predicted cross section significantly, and the data show a secondary maximum at 70° not seen in the well-established $l = 4$ level at 4.026 MeV (Fig. 10). Further, an $l = 4$ assignment is clearly inconsistent with the data at $E_d = 7.5$, 9, and 10 MeV. Neither assignment
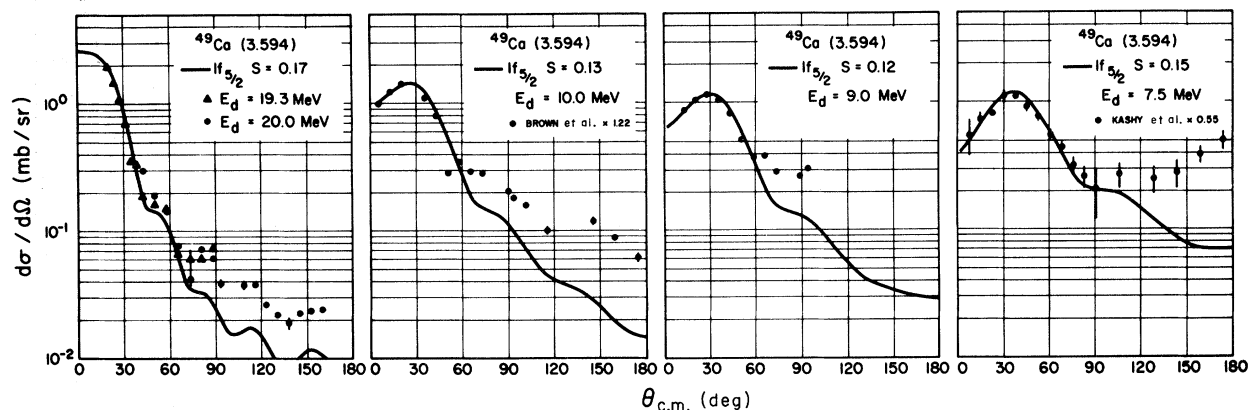
FIG. 9. Angular distributions of protons populating the 3.594 MeV state. The data at 7.5 and 10 MeV are taken from Refs. 1 and 11, renormalized as indicated. The data at 9 and 19.3+20 MeV are from the present measurement. The solid curves represent the DWBA predictions using AV GEOM parameters, with spectroscopic factors as indicated.

produces consistent spectroscopic factors. At 20 MeV, an $l = 3$ curve can reproduce the dip at $0°$ and the secondary maximum at 70°, but only if an $f_{7/2}$ "effective binding energy" of 9.9 MeV is used, as suggested by Sherr et al.[25] However, since the actual separation energy for the 3.364 MeV level is only 1.8 MeV, the amplitude of the $f_{7/2}$ wave function at the nuclear surface is much too small, producing an unrealistically large spectroscopic factor. Viewing Fig. 11, we note that the experimental data show a consistent trend with bombarding energy, but we conclude that we cannot fit that trend with our DW prescription. Canada et al.[5] have used our earlier[13] (and tentative) assignment of $l = 3$ or 4 assignment in limiting the spin-parity assignment for the 3.364 MeV level to $\frac{7\pm}{2}, \frac{9+}{2}$. In view of our withdrawal of this assignment, it would appear that an $E2$ assignment to the γ ray from the $\frac{9+}{2}$ 4.026 MeV level to the 3.364 MeV state would be possible, permitting also the possibility of $\frac{5+}{2}$ character to the latter level.

2. 3.875 MeV level

For this level the forward angle data taken at $E_d = 20$ MeV and displayed in Fig. 11 suggest $l = 4$. Brown et al.[11] make no l assignment to this transition at $E_d = 10$ MeV, although an $l = 4$ assignment could be supported by our DWBA prediction for that energy. But the 9 MeV data in Fig. 11, though limited, are clearly inconsistent with that assignment. Unfortunately, this state was not observed at 7 MeV. The 9 MeV data could be fitted by $l = 1$, but an $l = 1$ assignment is inconsistent with both the 10 and 20 MeV data at forward angles. Canada et al.[5] have noted that our earlier tentative assignment[13] of $l = 4$ to this transition is incompatible with the decay scheme. We agree, and note the danger of accepting the position of the maximum

of a single angular distribution to a weakly populated state as a definitive basis for an l assignment. The γ ray studies[5] offer no positive suggestions for spin and parity of the 3.875 MeV level. It is interesting to note that the transitions populating the 3.364 and 3.875 MeV levels show very similar angular distributions at 20 MeV and behave quite differently from each other at 9 and 10 MeV.

We conclude that for both of the anomalous transitions the data do not permit assignments of definite angular momentum transfer from DWBA analyses. It is conceivable that in each case the finite energy resolution is masking a doublet whose components vary differently with bombarding energy; however, the energy separation of the individual levels must be less than 15 keV. We have accounted for all peaks observed, and have observed all expected contaminant peaks. No evidence of splitting is seen in this or in earlier experiments; the consistency of the ^{49}Ca excitation energies listed in Table I does not suggest the existence of doublets, with the possible exception of the 3.364 MeV state. In any case, the distinction between the normal transitions and those populating the 3.364 and 3.875 MeV levels is clear experimentally.

F. Remaining transitions: 4.769, 4.788, and 4.904 MeV states

For these transitions, the information available is considerably less than for the others; consequently we have not made l assignments to the corresponding states.

As indicated in Fig. 12, for the transition populating the 4.769 MeV state, the proton group could not be extracted from contaminant groups at the crucial forward angles at $E_d = 20$ MeV. The transition has not been observed at other energies.
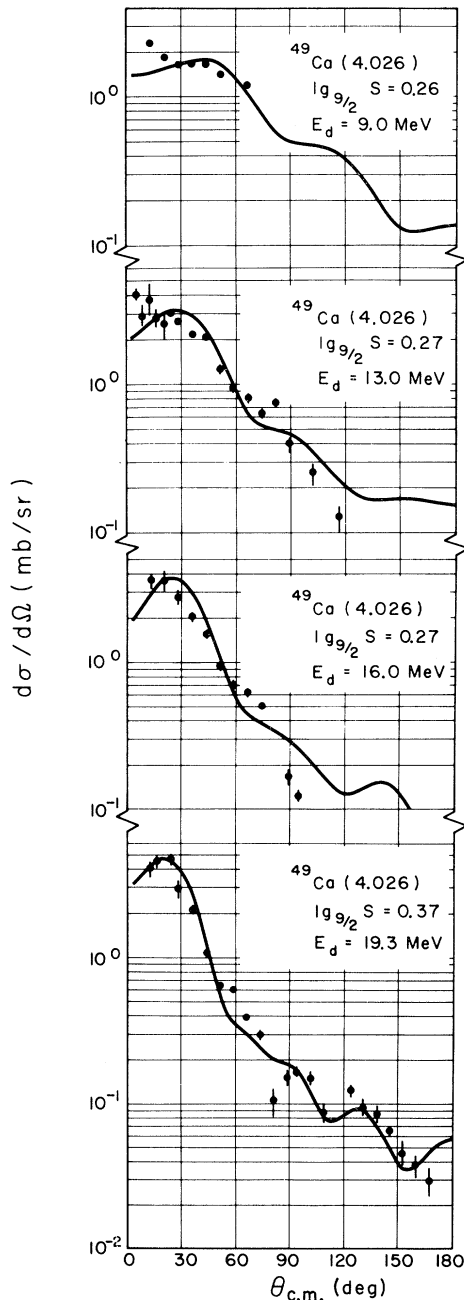
FIG. 10. Angular distributions of protons populating the 4.026 MeV state. The solid curves are DWBA predictions using the AV GEOM parameters, with spectroscopic factors as indicated.

For the protons populating the 4.788 MeV state, no DWBA curve fits very well. An $l = 4$ curve is sketched in Fig. 12 only for the sake of comparison; it follows the forward angle trend, but falls considerably below than the data beyond the forward maximum. At $E_d = 9$ MeV interference from contaminants obscured the proton group corre-

sponding to this level. The transition has not been observed at other energies.

The 4.904 MeV level has been observed earlier in the 10 MeV experiment.[11] In the present study, data of poor statistical quality were obtained at $E_d = 9$ MeV; within 30% random fluctuations they indicated a cross section of ~80 μb over the angular range 12.5–55°. At $E_d = 10$ MeV, the authors of Ref. 11 indicated a tentative $l = 4$ assignment, though their two forward angle points were substantially higher than their DWBA prediction (or ours, it may be added). Data at $E_d = 20$ MeV, shown in Fig. 12, is not fitted very well by any l; the $l = 4$ curve therein is sketched solely for purposes of comparison. Canada et al.[5] have suggested a spin of $\frac{7}{2}^+$ or preferably $\frac{9}{2}^+$; either assignment is compatible with $l = 4$, and indeed, the spectroscopic factors of Table II are compatible with $l = 4$. However, the $l = 4$ fit to the 20 MeV angular distributions shares the same difficulties as the $l = 4$ fit to the 4.788 MeV state. We do not believe the present evidence for an $l = 4$ assignment to be convincing.

V. STRUCTURE OF ^{49}Ca

The location of the single-particle states of ^{49}Ca have been well established by observation of the allowed transitions in the single-nucleon transfer experiments.[1-4] The onset of the next level of structural complexity is expected at about 3 MeV excitation,[5] and originates from promotion of a core nucleon to an unfilled orbital, forming a two-particle–1-hole state. Identification of the 2p-1h states is important; it could, in principle, be established by studying the allowed transitions in the (t, p) reaction on ^{47}Ca, or the (p, d) reaction on ^{50}Ca; unfortunately, these targets are not available. The identifications must be argued indirectly by showing that the energies, the spins, and parities of individual ^{49}Ca states, and the intensities with which they are populated in the (d, p) reaction, are consistent with a specific 2p-1h configuration. The formation of 2p-1h states in ^{49}Ca by a direct single-neutron transfer reaction on a 0p-0h ^{48}Ca ground state is forbidden. However, the one-step reaction can proceed by virtue of admixtures of a single-particle component in the final ^{49}Ca state, or via a 2p-2h component in the initial ^{48}Ca state. Estimates of such mixtures[5,26] suggest they are not large. Therefore, it is reasonable to consider the forbidden transitions here reported as indeed populating 2p-1h states through such admixtures.

Just as the single-particle states of ^{49}Ca are formed by coupling neutrons in successive shell-model orbits to the 0p-0h ^{48}Ca ground state, so
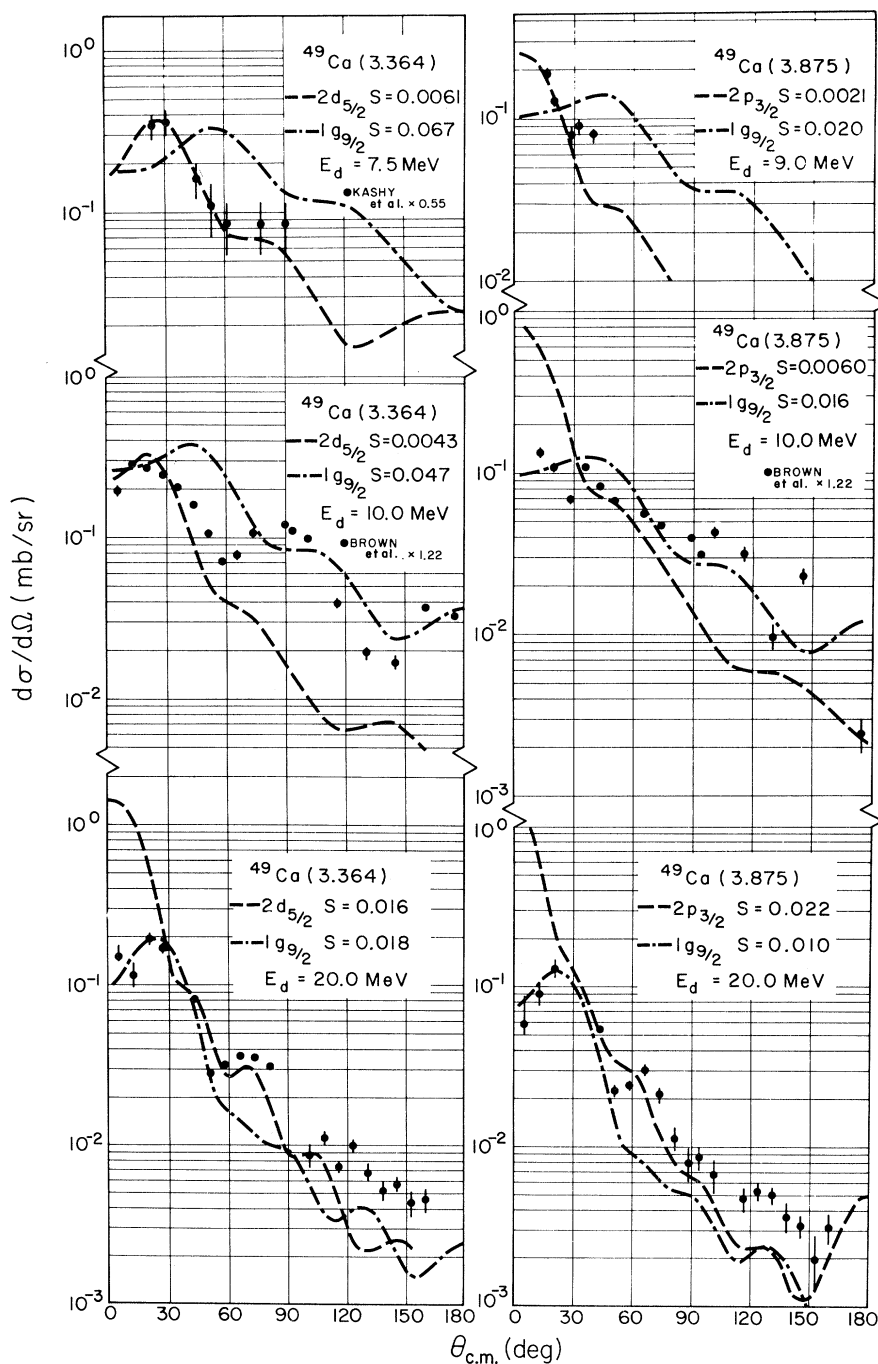
FIG. 11. Angular distributions of protons populating the 3.364 and 3.875 MeV states. The data at 7.5 and 10 MeV are those of Refs. 1 and 11, renormalized as indicated. The DWBA curves, calculated using AV GEOM parameters, are drawn only for purposes of illustration, and do not represent assignments.

2p-1h states can be formed by coupling a neutron to the 1p-1h and 2p-2h configurations of excited states of ^{48}Ca, as suggested in Fig. 13. (It is also useful to think of the 2p-1h states of ^{49}Ca as constructed from ^{50}Ca states by coupling neutron holes to the two-neutron configurations thereof.[5]) The

first excited state of ^{48}Ca is the 2^+ level at 3.83 MeV, dominated by the $f_{7/2}^{-1}p_{3/2}$ configuration. Coupling a $p_{3/2}$ neutron would form a triplet of spins $\frac{7}{2}^-$, $\frac{5}{2}^-$, and $\frac{3}{2}^-$ in ^{49}Ca. Canada et al.[5] have identified the $\frac{5}{2}^-$ level at 3.594 MeV with the corresponding member of this triplet. We note that
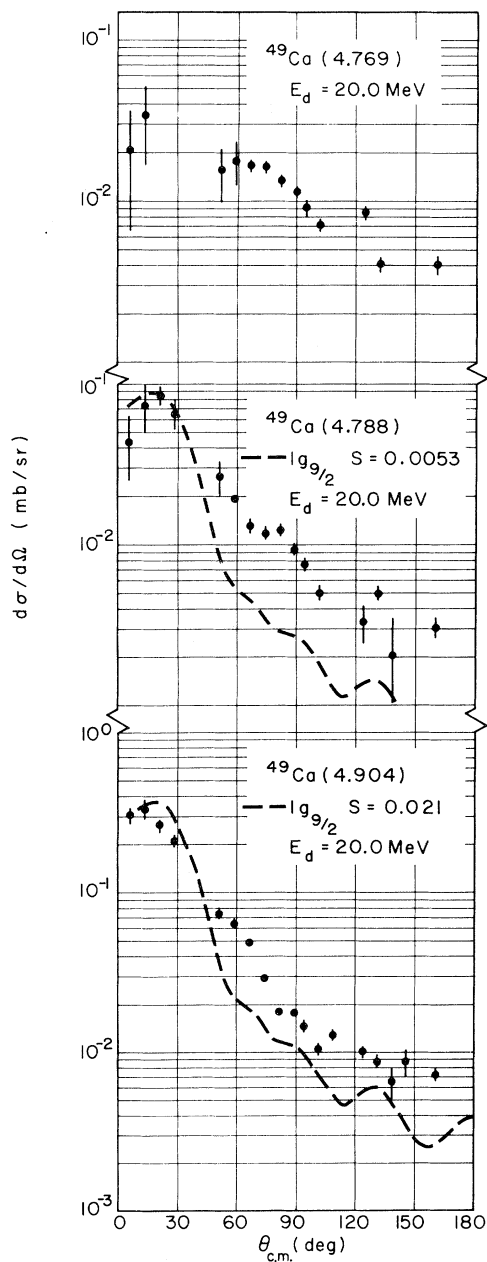
FIG. 12. Angular distributions of protons populating the 4.769, 4.788, and 4.904 MeV states in ^{49}Ca. The DWBA curves are drawn only for purposes of illustrations and do not represent assignments.

FIG. 13. Core-coupling model for ^{49}Ca. The known ^{48}Ca states are shown to the left, the square brackets indicating the principal components of the wave functions suggested in Ref. 26. The multiplets indicated in the center column can be formed by coupling a $2p_{3/2}$ or $1f_{7/2}$ neutron to the appropriate excited ^{48}Ca state. Identifications with the known ^{49}Ca spectrum on the right are suggested by the dashed lines.

the total $f_{5/2}$ single particle strength appears to be distributed between this state and the main fragment at 4.007 MeV, and suggest that this coupling completely accounts for the observed fragmentation of the $f_{5/2}$ strength. Canada et $al.$ have also suggested that the 3.364 MeV level be identified with the $\frac{7}{2}^-$ component and the 3.875 MeV level with the $\frac{3}{2}^-$ member. However, because the $\frac{3}{2}^-$ member of the triplet is the only $l = 1$ state ex-
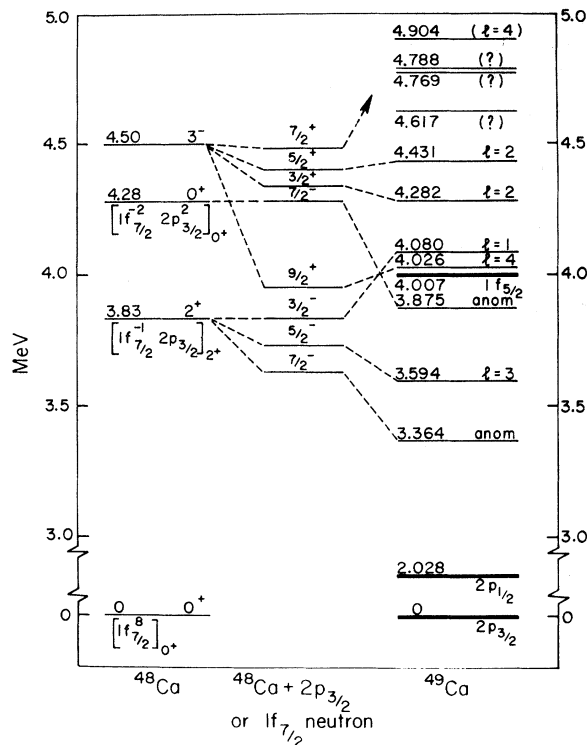
pected in this region, we prefer to identify it with the 4.080 MeV state assigned $l = 1$ in Sec. IV. The recognizable DWBA pattern observed for the 3.594 and 4.080 MeV states signifies the existence of appreciable $f_{5/2}$ and $p_{3/2}$ admixtures in their wave functions. The 3.364 MeV state, taken as the $\frac{7}{2}^-$ member, is populated by an anomalous transition. This fact we take to indicate the lack of an appreciable $f_{7/2}$ admixture accessible via the main 0p-0h component of the target wave function. This state is evidently populated through the small 2p-2h components of the ^{48}Ca ground state, accounting for its low cross section. The anomalous behavior of the angular distributions may result from interference with a two-step process in which inelastic scattering to the 2^+ state is followed by an $l = 1$ neutron transfer.

A positive parity quadruplet can be formed by coupling the strongly collective 4.51 MeV 3^- ^{48}Ca state to a $p_{3/2}$ neutron (see Fig. 13). Canada et $al.$[5] apply the weak-coupling scheme outlined by Mottelson[27] to calculate the admixture of this particle-vibration multiplet with the single-particle

states. The calculated energy splittings and spectroscopic factors support the identification[5] of the 4.026 MeV ($l=4$) state with the $\frac{9}{2}^+$ member of the multiplet, the 4.282 MeV ($l=2$) state with the $\frac{3}{2}^+$ member, and the 4.431 MeV ($l=2$) state as the $\frac{5}{2}^+$ member. In each case, the d,p transition proceeds from the principal component of the ^{48}Ca ground state via the admixture of the appropriate single-particle state. There is no clear identification of the $\frac{7}{2}^+$ member of the multiplet, but the 4.769, 4.788, or 4.904 states are possible candidates. Another of these three may result from mixing the $g_{9/2}$ state with a member of the next $3^- \otimes p_{3/2}$ multiplet, expected at about 5.4 MeV in ^{49}Ca.

An additional 2p-1h state is expected to result from coupling an $f_{7/2}$ neutron to the 2p-2h 0^+ state of ^{48}Ca at 4.28 MeV. Canada $et\ al.$[5] have suggested the 4.080 MeV level as a candidate, but this is not compatible with our $l=1$ assignment. We would suggest instead the 3.875 MeV level. The anomalous transition populating this level may arise from the fact that a direct neutron transfer can operate only through the small 2p-2h components of the ^{48}Ca ground state, again with possible interference from a two-step process.

VI. COMMENTS

In the present study we have found a surprisingly simple DWBA model to be capable of accounting for not only the angular dependence of single-particle (allowed) and non-single-particle (forbidden) transitions, but also for their energy dependence over a large range. Although nonlocal, finite-range, and deuteron-breakup effects are not included, the spectroscopic factors are consistent, providing we have correctly renormalized two earlier measurements.[1,11] However, we do not suppose these DWBA parameters to be unique.

Fixed initially by data in the range $E_d=13-20$ MeV, the quality of the fits begins to deteriorate at $E_d=7.5$ MeV. Bogaards and Roy[9] have used a considerably more sophisticated model including full spin-orbit effects to account for the transition to the $2p$ states for $E_d=2.5-5.5$ MeV. It would be quite interesting to explore whether their model could account for the behavior (including j dependence) at higher energies, especially if polarization data become available.

The particle-core coupling model originally applied to ^{49}Ca by Canada $et\ al.$[5] appears to be capable of accounting for all the 2p-1h states observed below 4.5 MeV; however, the roles assigned by these authors to the 3.875 and the 4.080 MeV states must be reversed. The spectroscopic information now available would appear to justify a more sophisticated calculation of the particle-core coupling than has been published to data for ^{49}Ca. For the anomalous transitions, the proposed structure is qualitatively consistent with the weakness of the transitions in that the direct interaction would proceed through small fragments of the ground-state wave function, but the angular distributions of Fig. 11 require either a more complex final-state wave function or a more complex reaction mechanism, similar to that suggested in Ref. 28.

*Work supported by U.S. Atomic Energy Commission Contract No. AT(11-1)-3074.

†Present address: Science Magazine, Washington, D.C.

[1]E. Kashy, A. Sperduto, H. A. Enge, and W. W. Buechner, Phys. Rev. 135, B865 (1964).

[2]J. R. Erskine, A. Marinov, and J. P. Schiffer, Phys. Rev. 142, 633 (1966).

[3]R. Santo, R. Stock, J. H. Bjerregaard, O. Hansen, and O. Nathan, Nucl. Phys. A118, 409 (1968); Nucl. Phys. (Erratum) A139, 711 (1969).

[4]D. Schmitt and R. Santo, Z. Phys. 233, 114 (1970).

[5]T. R. Canada, C. Ellegaard, and P. D. Barnes, Phys. Rev. C 4, 471 (1971).

[6]T. A. Belote, W. E. Dorenbusch, and J. Rapaport, Nucl. Phys. A120, 401 (1968).

[7]S. A. Anderson, O. Hansen, R. Chapman, and S. Hinds,

Nucl. Phys. A120, 421 (1968); Nucl. Phys. (Erratum) A139, 707 (1969).

[8]G. Brown, A. Denning, and A. E. Macgregor, Nucl. Phys. A153, 145 (1970).

[9]J. J. W. Bogaards and G. Roy, Nucl. Phys. A160, 289 (1971).

[10]J. Rapaport, A. Sperduto, and M. Salomaa, Nucl. Phys. A197, 337 (1972).

[11]G. Brown, A. Denning, and J. G. B. Haigh, Nucl. Phys. A225, 267 (1974).

[12]W. T. Pinkston and G. R. Satchler, Nucl. Phys. 72, 641 (1965).

[13]W. D. Metz, W. D. Callender, C. F. Maguire, D. G. Kovar, L. J. McVay, and C. K. Bockelman, Bull. Am. Phys. Soc. 16, 150 (1971).

[14]D. G. Kovar, C. K. Bockelman, W. D. Callender, L. J.

McVay, C. F. Maguire, and W. D. Metz, Wright
Nuclear Structure Laboratory Internal Report No. 49,
1970 (unpublished).

[15]P. Spink and J. R. Erskine, Argonne National Labora-
tory, Physics Division Informal Report No. PHY-
1965B, 1965 (unpublished).

[16]E. H. Auerbach (private communication).

[17]W. D. Metz, Ph.D. thesis, Yale University, 1972 (un-
published).

[18]P. D. Kunz (private communication).

[19]R. J. Peterson, Phys. Rev. 170, 1003 (1968).

[20]P. Schwandt and W. Haeberli, Nucl. Phys. A123, 401
(1969).

[21]A. Marinov, L. L. Lee, Jr., and J. P. Schiffer, Phys.
Rev. 145, 852 (1966).

[22]C. M. Perey and F. G. Perey, Phys. Rev. 132, 755
(1963).

[23]C. Glashausser and M. E. Rickey, Phys. Rev. 154,
1033 (1967).

[24]T. T. S. Kuo and G. E. Brown, Nucl. Phys. A114, 241
(1968).

[25]R. Sherr, B. F. Bayman, E. Rose, M. E. Rickey, and
C. G. Hoot, Phys. Rev. 139, B1272 (1965).

[26]P. Federman and S. Pittel, Nucl. Phys. A155, 161
(1970).

[27]B. R. Mottelson, in Proceedings of the International
Conference on Nuclear Structure, edited by J. Sawada
[J. Phys. Soc. Jpn. Suppl. 24 (1968)], p. 96.

[28]S. Mukherjee and R. Shyam, Phys. Rev. C 11, 476
(1975).